RESEARCH ARTICLE

American Journal of Botany

Within-crown plasticity in leaf traits among the tallest conifers

Alana R. O. Chin[1,2,4] and Stephen C. Sillett[3]

Manuscript received 11 July 2018; revision accepted 30 November 2018.

[1] Department of Natural Resources, American River College, 4700 College Oak Drive, Sacramento, CA 95841, USA

[2] Present address: Department of Plant Sciences, University of California Davis, 1 Shields Ave, Davis, CA 95616, USA

[3] Department of Forestry and Wildland Resources, Humboldt State University, 1 Harpst Street, Arcata, CA 95521, USA

[4] Author for correspondence (e-mail: alanaroseo@gmail.com)

Citation: Chin, A. R. O. and S. C. Sillett. 2019. Within-crown plasticity in leaf traits among the tallest conifers. *American Journal of Botany* 106(2): 174–186.

doi:10.1002/ajb2.1230

PREMISE OF THE STUDY: Leaves are the sites of greatest water stress in trees and a key means of acclimation to the environment. We considered phenotypic plasticity of *Pseudotsuga menziesii* leaves in their ecological context, exploring responsiveness to natural gradients in water stress (indicated by sample height) and light availability (measured from hemispherical photos) to understand how leaf structure is controlled by abiotic factors in tall tree crowns.

METHODS: After measuring anatomy, morphology, and carbon isotope composition ($\delta^{13}C$) of leaves throughout crowns of *P. menziesii* >90 m tall, we compared structural plasticity of leaves among the three tallest conifer species using equivalent data from past work on *Sequoia sempervirens* and *Picea sitchensis*.

KEY RESULTS: Leaf mass per projected area (LMA) and $\delta^{13}C$ increased and mesoporosity (airspace/area) decreased along the water-stress gradient, while light did not play a detectable role in leaf development. Overall, leaves of *P. menziesii* were far less phenotypically responsive to within-crown abiotic gradients than either *P. sitchensis*, whose leaves responded strongly to light availability, or *S. sempervirens*, whose leaves responded equally strongly to water stress.

CONCLUSIONS: *P. menziesii* maintain remarkably consistent leaf structure despite pronounced vertical gradients in abiotic factors. Contrasting patterns of leaf structural plasticity underlie divergent ecological strategies of the three tallest conifer species, which coexist in Californian rainforests.

KEY WORDS Cupressaceae; functional traits; hydraulic conductivity; leaf anatomy; phenotypic plasticity; *Picea sitchensis*; Pinaceae; *Pseudotsuga menziesii*; *Sequoia sempervirens*; tree height.

The tallest reliably measured tree, according to historical and contemporary records, was a 126 m tall Douglas-fir [*Pseudotsuga menziesii* (Mirb.) Franco; Pinaceae] felled in British Colombia over a century ago (Carder, 1995). To be tallest among all species necessitates a singular ability to outgrow the competition while maintaining water supply to treetop leaves. Within plant stems, gravity exerts 0.0098 MPa m^{-1} on the water column, causing a linear decline in leaf water potential (Ψ) with increasing height even when the water column is static (Zimmermann, 1983). To mitigate the chronic water stress attending great height, *P. menziesii* invests in osmotic adjustment of the water status in living cells, but the vertical gradient in Ψ cannot be overcome (Meinzer et al., 2008; Woodruff and Meinzer, 2011). The impact of gravity can be detected by the increased fraction of ^{13}C in treetop leaves, which is a signature of stomatal limitation due to reduced aperture or early closure (Farquhar et al., 1989; Hultine and Marshall, 2000). Light availability also increases with height, ranging from <20% in the lower crown to full exposure at the treetop in emergent forest trees (Oldham et al., 2010; Ambrose et al., 2016). Evolution of tall trees involved a balance of stem persistence and rapid elongation (King, 1990; Niklas, 1997; Falster and Westoby, 2003), and the tallest species are those possessing broad physiological tolerance of water stress as well as an ability to gain height rapidly when not shaded. The capacity of leaves to acclimate to the wide variety of conditions encountered along the height gradient is critical to the development of

crowns >50 m deep in the four tallest species (*Eucalyptus regnans*, *Picea sitchensis*, *P. menziesii*, *Sequoia sempervirens*), and this phenotypic plasticity has important implications for forest structure and species coexistence (Sillett et al., 2015; Van Pelt et al., 2016; Chin and Sillett, 2017).

Within-crown variation in water and light availability induces leaf-level responses in conifers that reflect a combination of biophysical constraints on leaf growth and functional traits supporting both water stress tolerance and photosynthetic efficiency (Niinemets and Kull, 1995a,b; Niinemets, 2002; Cescatti and Zorer, 2003; Ishii et al., 2008; Ambrose et al., 2009; Gebauer et al., 2011, 2012, 2015). In all tall conifers studied to date, leaf length decreases while leaf mass per projected area (LMA) increases with height. Shortness and high density of treetop leaves have been attributed to constraints on cellular expansion resulting from gravity's effect on Ψ (Marshall and Monserud, 2003). For cells to elongate, turgor must be sufficiently high to breach cell wall yield thresholds (Cosgrove, 1993, 2000; Wu et al., 2005). Turgor in living cells is limited under conditions of low xylem Ψ, which in turn limits leaf length not only in trees, but also in other plants facing chronic water stress, forcing leaves to expand during nightly Ψ peaks (Boyer, 1968; Van Volkenburgh and Boyer, 1985; Boyer and Silk, 2004). The minimum phloem loading required for osmotically driven export of photosynthate over a given distance sets limits on maximum efficient leaf length in conifers, where a greater radius of phloem tissue can sustain transport through longer leaves without stagnation at the leaf tip (Rademaker et al., 2017). Nonetheless, ecological constraints may result in a realized leaf length below the maximum predicted given available phloem. For example, total radius of phloem tissue in *P. sitchensis* increases with light availability, and yet leaf length still decreases with height (Chin and Sillett, 2017). In *P. menziesii*, a seasonal pulse of various osmotica fits the timing of a reduction in branch-level nonstructural carbohydrate (NSC) stores from bud-swell through the period of leaf elongation, implying that turgor, and thus maximum treetop leaf length, are tied to NSC release (Billow et al., 1994; Woodruff et al., 2008a; Woodruff and Meinzer, 2011).

Beyond constraints on size, conifer leaves exhibit a high degree of within-crown plasticity in anatomical traits, consistently including expansion of transfusion tissue area with increased sampling height (Oldham et al., 2010; Azuma et al., 2015; Chin and Sillett, 2016, 2017). Transfusion tissue of conifers is a collection of tracheids involved in radial water transport and capacitance that temporarily collapse under hydraulic stress to protect adjacent xylem in some, if not all, species (Hu and Yao, 1981; Brodribb and Holbrook, 2005; Ishii et al., 2014; Zhang et al., 2014; Azuma et al., 2015). In many species, parenchyma cells are interspersed among transfusion tracheids and may serve to retrieve solutes from the transpiration stream and deliver photosynthate to phloem, but distribution of these two cell types across the vertical gradient has not been investigated (Hu and Yao, 1981; Canny, 1993; Liesche et al., 2011). Treetop leaves of *P. menziesii* up to 65 m tall in Washington are shorter and narrower with thicker cuticles, more astrosclereids, lower stomatal density, and smaller, fewer, and more embolism-resistant xylem tracheids than leaves lower in the crown (Apple et al., 2002; Woodruff et al., 2004, 2008a,b, 2010). In addition to functional traits to cope with water stress and osmotic adjustments of cell turgor, many plants, including *P. menziesii*, can raise leaf Ψ above the gravitational potential gradient through foliar uptake of water (Burgess and Dawson, 2004; Limm et al., 2012).

Among the three tallest conifer species, *P. menziesii* has the broadest geographic range, extending from British Columbia to Mexico and from the Coast and Cascade Ranges to the Rocky Mountains. The other two tallest conifers, *Sequoia sempervirens* and *Picea sitchensis*, are restricted to the temperate coast and have fewer ecological associations (Hardin et al., 2001; Sawyer et al., 2009). In California alone, there are three recognized *P. menziesii*-dominated vegetation alliances containing >100 distinct associations, yet only one alliance with 19 associations is recognized for *S. sempervirens*, and one alliance with six associations is recognized for *P. sitchensis* (Sawyer et al., 2009). Illustrative of its ecological breadth, *P. menziesii* occurs in forest communities defined by such diverse species as *Pinus ponderosa*, *Abies lowiana*, *Chamaecyparis lawsoniana*, and *Acer macrophyllum* (Sawyer et al., 2009). In the rainforests dominated by *S. sempervirens* in northern California, *P. menziesii* and *P. sitchensis* >90 m tall coexist with even taller redwoods (Chin and Sillett, 2017).

Although the tallest conifers have similar patterns of crown development—increasing structural complexity as original tops and branches are damaged and replaced—*S. sempervirens* is far more fire- and decay-resistant and longer-lived than *P. sitchensis*, while *P. menziesii* is intermediate in these characteristics (Van Pelt, 2001; Van Pelt and Sillett, 2008; Sillett et al., 2018). Whereas *S. sempervirens* has leaves that respond anatomically to the within-crown water-stress gradient, leaf development of *P. sitchensis* is primarily controlled by light availability (Oldham et al., 2010; Chin and Sillett, 2017). Which of these environmental factors is a stronger driver of plasticity in *P. menziesii* leaves is unknown. Here we examined leaf anatomy and morphology of six *P. menziesii* trees up to 97 m tall—30 m taller than any individuals of this species previously studied at the leaf level—alongside existing leaf-trait data from *P. sitchensis* and *S. sempervirens* trees up to 97 and 113 m tall, respectively (Oldham et al., 2010; Chin and Sillett, 2017). We assessed the impacts of light and water availability on leaf structural plasticity in the tallest conifers to explore how contrasting strategies for coping with extreme height allow species with different growth rates and investments in longevity to reach comparable size.

MATERIALS AND METHODS

Study locations and trees

No living *P. menziesii* trees >100 m tall are known, but trees >90 m occur in forest reserves from British Colombia to California. We selected five trees 91–97 m tall (trees 1–5, N = 46 samples) from Prairie Creek Redwoods State Park, California for detailed study (41.4034°N, 124.0299°W). This reserve protects the only known forest with three species >90 m tall (i.e., *S. sempervirens*, *P. sitchensis*, *P. menziesii*). We also collected samples from a 92 m tall *P. menziesii* tree (tree 6, N = 8 samples) in Olympic National Park, Washington (47.8609°N, 123.9348°W) to clarify differences between our results from trees 1–5 and those of previous studies on ~60 m tall trees farther north, where leaves varied strongly along the vertical gradient (Woodruff et al., 2004, 2008a). Tree 6 from Washington was also used to obtain longitudinal sections and leaf surface imprints for examination of mesophyll structure and stomatal patterns. The six individuals used here correspond to trees 26–30 and 15 in a recent study of *P. menziesii* (Sillett et al., 2018).

Sample collection and preparation

Trees were climbed with standard rope techniques to collect samples at 5–10 m intervals from a range of crown positions to represent the diversity of within-crown light environments and reduce the correlation between light availability and height (Fig. 1). We measured sample height with a tape dropped to average ground level, determined as halfway between highest and lowest points where the trunk meets soil beneath debris. For trees 1–5, light availability was measured via hemispherical photographs taken directly above each sample using a camera on a self-leveling mount. We analyzed photographs using WinScanopy (Régents Instruments, Nepean, Ontario, Canada) to compute total site factor (TSF), the proportion of direct and indirect solar radiation relative to open sky. We chose TSF over direct measurements of radiation because it is representative of year-round light availability in evergreen forests and independent of time of day or season.

Immediately after collection, shoots were re-cut underwater and kept hydrated until being fixed for 2 weeks in formalin–propionic acid (FPA). One fixed leaf per sample was embedded in paraffin, affixed to a hardwood block, and sectioned transversely at mid-leaf with a rotary microtome. After mounting on glass slides, leaf sections were stained with Walker's Sam stain: Bismark brown, Weigert's iron hematoxylin, phloxine, and clove oil saturated with a mixture of fast green and orange G. We preferred this complex stain because it very clearly differentiates tissues, making image analysis easier and allowing us to infer tissue composition. Individual leaves from tree 6 were sectioned green without fixation to assess mesophyll structure more effectively without artefacts caused by fixation and dehydration (Chin and Sillett, 2017).

All leaves were cut to approximately 10 μm thickness. Leaves for green transverse sections were placed directly in the microtome sample holder, while leaves for longitudinal sections were first placed on hardwood blocks and coated with Original Super Glue (method described by Chin and Sillett, 2017). To embed samples in Super Glue, we treated the block surface with liquid glue, positioned the leaf on the block when it became tacky, and added additional glue sufficient to cover the leaf in a droplet. When fully dry, these glue-embedded samples were sectioned with a sliding microtome while carefully keeping the exposed leaf surface wet with a brush. The Super Glue does not penetrate the leaf, heat up, or damage cells while curing, and coated leaves retain their moisture. We also made acrylic resin (nail polish) imprints of both adaxial and abaxial leaf surfaces, placing nail polish directly on the slides, setting leaves in the polish, and then carefully removing leaves from the slide surface when dry. All sections and imprints were photographed at 40× and analyzed with ImageJ software, except surface imprints, which were photographed at 40× to measure stomatal density and at 400× to measure guard cell length.

Subsamples from all shoots collected (trees 1–6) were also scanned, dried, and weighed for calculation of LMA or ground to powder and used for analysis of $\delta^{13}C$. Samples from trees 1–5 were analyzed at the Colorado Plateau Stable Isotope Laboratory (Flagstaff, AZ, USA), and samples from tree 6 were analyzed at the UC Davis Stable Isotope Facility (Davis, CA, USA). Both facilities report carbon isotope ratios relative to the same international standard, Vienna PeeDee Belemnite. We selected anatomical and morphological traits responsive to variation in light, water availability, or both in other tall species, including some previously measured in shorter *P. menziesii* trees from other regions.

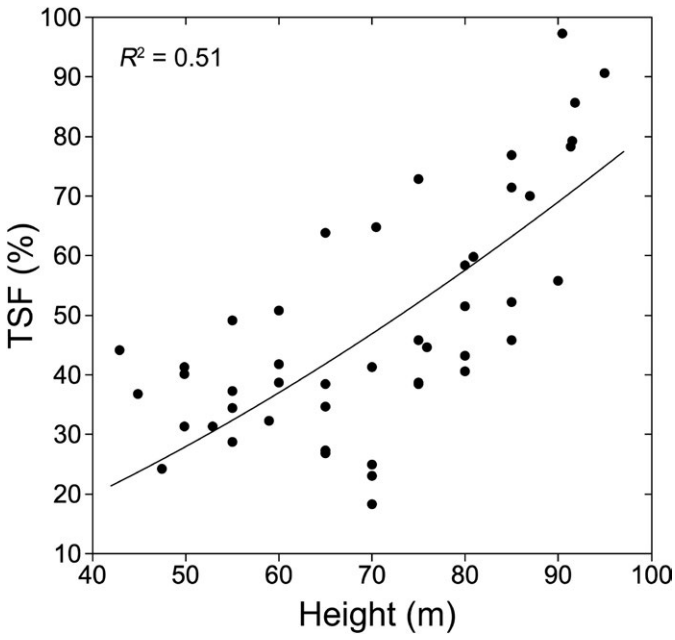

FIGURE 1. Relationship between light availability (TSF) and sample collection height in the crowns of *Pseudotsuga menziesii* trees 1–5. Line shows best power function. Goodness of fit (R^2) value is for linear correlation between power-transformed height versus measured TSF.

Data analysis

To separate effects of within-crown gradients on *P. menziesii* leaf anatomy, we modeled 18 leaf traits as functions of multiple predictors representing water stress and light availability (Table 1). We used TSF as the predictor of light availability, height as an index of maximum water potential (barring foliar uptake), and $\delta^{13}C$ to express chronic water stress as indicated by limited stomatal openness (Farquhar et al., 1989; Chin and Sillett, 2016). For tree 6, we used linear regression to examine trends in six stomatal and mesophyll traits against height and $\delta^{13}C$ (Table 1).

Starting with a saturated model (height, $\delta^{13}C$, and TSF), we used a stepwise model-selection procedure to remove each term sequentially. Corrected Akaike information criterion (AIC_c) was computed at each step to determine the value of adding back terms removed at previous steps. For each trait, we retained the top three models and assigned a relative likelihood (Akaike weight) for comparison. Reducing the candidate set to models with useful predictive ability, we discarded those with non-intercept parameters that had standard errors more than half the mean estimate. Nearly all leaf traits were represented by a single ecological model (or none) following the selection procedure, but when two models remained, they were compared based on goodness of fit (R^2) and relative likelihood (recalculated Akaike weights).

We used principal components analysis (PCA) to examine the leaf-trait space occupied by three co-occurring tall species, adding five *S. sempervirens* trees (data from Oldham et al., 2010) and five *P. sitchensis* trees (data from Chin and Sillett, 2017) to our *P. menziesii* matrix. After excluding redundant variables (e.g., including LMA but not mass or area), nine traits common to all species remained (Table 2). PCA was performed on the combined matrix (153 leaves, 9 traits; Chin and Sillett, 2018) using a correlation cross-products matrix, and statistically significant principal components were

TABLE 1. Measured anatomical and morphological traits of *Pseudotsuga menziesii* leaves. Traits in bold type were used in multiple regression models.

Leaf trait	Units	Trees	Method[a]
Total area of transverse section	mm^2	1-6	¤ §
Leaf length	mm	1-6	✧
Width	mm	1-6	¤ §
Thickness	mm	1-6	¤ §
Perimeter of transverse section	mm	1-6	¤ §
Cuticle thickness	mm	1-6	¤ §
Epidermal thickness	mm	1-6	¤ §
Valley depth between epidermal cells	mm	1-6	¤ §
Xylem area	mm^2	1-6	¤ §
Phloem area	mm^2	1-6	¤ §
Transfusion tissue area	mm^2	1-6	¤ §
LMA (leaf mass per area)	$g\ m^{-2}$	1-6	✧
Distance between endodermis and abaxial epidermis	mm	1-6	¤ §
Distance between endodermis and adaxial epidermis	mm	1-6	¤ §
Maximum distance between endodermis and epidermis	mm	1-6	¤ §
Maximum endodermal thickness	mm	1-6	¤ §
Number of plications per spongy mesophyll cell	count	1-6	¤ §
Vascular bundle area (everything inside endodermis)	mm^2	1-6	¤ §
Dry mass	g	1-6	✧
Projected area	mm^2	1-6	✧
Number of transfusion tracheids	count	1-5	¤
Abaxial stomata per mm	count	6	°
Guard cell length	mm	6	°
Stomatal pore index (SPI)	stomatal density × guard cell length	6	°
Number of mesophyll plates per mm	count	6	«
Connections per mesophyll plate	average count	6	«
Distance between mesophyll plates	mm	6	«
Mesoporosity	airspace (mm^2) / area (mm^2)	6	«

[a]Methods: § = green cross section, ¤ = paraffin embedded cross section, ° = resin imprint, « = green longitudinal section, and ✧ = scanned / weighed.

identified via randomization tests (Peres-Neto et al., 2005). For meeting the assumption of multivariate normality, one trait (leaf cross-sectional area) was square-root-transformed before analysis. Skewness averaged 0.539 and kurtosis averaged 0.477 in the final matrix, and there was no pronounced bivariate nonlinearity. Using leaf scores along significant principal components as Cartesian coordinates, we calculated mean centroid distances for the three pairwise comparisons of species as well as trees 1–5 versus tree 6 of *P. menziesii*. PCA was performed in JMP (version 13, SAS Institute, Cary, NC, USA), except randomization tests performed in PC-ORD (version 6, McCune and Mefford, 2011).

TABLE 2. Correlations (*r*) between principal component scores and traits of 153 leaves (54 *P. menziesii*, 57 *S. sempervirens*, 42 *P. sitchensis*) after eigenvalues and variance explained for three significant principal components. Correlations in bold type were the strongest for each trait.

Trait	PC1	PC2	PC3
Eigenvalue	3.69	2.16	1.94
Variance explained (%)	41.0	24.0	21.6
Total cross-sectional area	**0.914**	−0.298	0.181
Width	**0.848**	−0.134	−0.450
Perimeter of cross section	**0.835**	−0.279	−0.423
Xylem cross-sectional area	**0.799**	0.464	−0.119
Phloem cross-sectional area	0.639	**0.679**	−0.050
Transfusion tissue cross-sectional area	0.261	**0.639**	0.570
Leaf length	−0.126	**0.778**	−0.132
LMA	0.263	0.026	**0.898**
Thickness	0.490	−0.533	**0.603**

Finally, we compared structure of *P. menziesii* leaves to other tall conifers using our previously published data on *S. sempervirens* (Oldham et al., 2010) and *P. sitchensis* (Chin and Sillett, 2017). Following the method of Valladares et al. (2006), we calculated plasticity using species-mean trait values from the highest and lowest samples from each of 5 trees per species as (maximum – minimum) / (maximum). Both mean plasticity across traits and plasticity of individual traits were calculated for each species.

RESULTS

Leaf anatomy and morphology

Height, not light availability, was the dominant predictor of leaf anatomical variation in *P. menziesii*, and we found suitable ecological models for 16 leaf traits (Table 3). Only three modeled traits—LMA, number of tracheids in transfusion tissue, and cuticle thickness—had $R^2 > 0.3$. Areas of xylem and phloem were the only traits best explained by light availability, and these only weakly (Table 3). Some traits poorly explained by predictors in trees 1–5 from California had a better fit to height and $\delta^{13}C$ in tree 6 from Washington (Table 4). Although leaf width was unrelated to any predictor in trees 1–5 (Table 3), 87% of leaf width variation was explained by $\delta^{13}C$ in tree 6 (Table 4). The PCA of nine traits among 153 leaves revealed strong segregation among species along PC2 (Fig. 2), which expressed variation in leaf length and vascular bundle size (Table 2). Substantial overlap among species occurred along PC1 and PC3 (Fig. 2), which expressed variation in leaf cross-sectional size and LMA, respectively (Table 2). Tree 6 clustered among its fellow *P. menziesii*, except for very low-LMA leaves from the lower crown and very short leaves from the upper crown (Fig. 2). Centroid distance between trees 1–5 and tree 6 (2.0) was considerably smaller than any centroid distance between species (3-pair mean = 3.6) using leaf scores along the three significant principal components.

Leaves of *P. menziesii* had a central longitudinal groove running down the exposed adaxial surface, a single vascular bundle within an endodermis, and stomata restricted to the abaxial leaf surface at all heights (Fig. 3A, B, D). The mesophyll was arranged into plates, and mesoporosity (airspace/mesophyll area) was closely related to height as were two traits driving the mesoporosity decrease—number of connections between mesophyll plates and maximum

TABLE 3. Multiple regression models for leaf traits of *Pseudotsuga menziesii* ranked top to bottom by goodness of fit (R^2). Selection criterion (AIC_c) and Akaike weight (w_i) listed for each model. Each parameter estimate is given with one standard error (SE).

						1st Predictor		2nd Predictor		Intercept	
Leaf trait	**Rank**	**Predictor(s)**	R^2	AIC_c	w_i	**Estimate**	**SE**	**Estimate**	**SE**	**Estimate**	**SE**
LMA	1	Height, $\delta^{13}C$	0.688	371	0.902	8.824E−01	1.848E−01	5.722E+00	2.177E+00	2.792E+02	6.934E+01
	2	Height	0.638	375	0.098	1.226E+00	1.393E−01	–	–	9.861E+01	9.977E+00
Number of transfusion tracheids	1	Height	0.402	337	1	5.004E−01	9.207E−02	–	–	8.504E+00	6.594E+00
Cuticle thickness	1	Height	0.328	−472	1	6.469E−05	1.395E−05	–	–	1.201E−03	9.987E−04
Vascular bundle area	1	Height	0.246	−349	1	2.026E−04	5.346E−05	–	–	1.389E−02	3.829E−03
Total area of transverse section	1	Height	0.215	229	1	−9.847E−02	2.837E−02	–	–	2.438E+01	2.032E+00
Number of plications per spongy mesophyll cell	1	$\delta^{13}C$	0.181	101	1	2.609E−01	8.374E−02	–	–	1.244E+01	2.293E+00
Distance between endodermis and adaxial epidermis	1	Height	0.176	−229	1	6.043E−04	1.954E−04	–	–	4.539E−02	1.399E−02
Epidermal thickness	1	Height	0.172	−412	1	8.106E−05	2.683E−05	–	–	1.325E−02	1.922E−03
Xylem area	1	Light	0.160	−526	1	1.684E−05	5.827E−06	–	–	2.035E−03	3.024E−04
Leaf length	1	Height	0.157	212	1	−6.764E−02	2.368E−02	–	–	2.226E+01	1.696E+00
Depth of adaxial groove	1	Height	0.153	−238	1	5.030E−04	1.784E−04	–	–	1.952E−02	1.278E−02
Transfusion tissue area	1	Height	0.131	−314	1	2.000E−04	7.761E−05	–	–	3.917E−02	5.558E−03
Phloem area	1	Light	0.122	−484	1	2.291E−05	9.264E−06	–	–	3.547E−03	4.808E−04
Valley depth between epidermal cells	1	Height	0.110	−489	1	2.730E−05	1.169E−05	–	–	2.758E−03	8.372E−04
Width	1	Height, $\delta^{13}C$	0.110	−98	1	2.513E−03	1.138E−03	−2.717E−02	1.341E−02	3.140E−01	4.271E−01
Perimeter of transverse section	1	Height	0.034	31	1	4.085E−03	3.303E−03	–	–	2.768E+00	2.366E−01

TABLE 4. Correlations (r) of anatomical traits with height and $\delta^{13}C$ for eight leaves of tree 6 from Washington. Two-tailed P-values are shown for each correlation. Correlations in bold type were the strongest for each trait.

	Height		$\delta^{13}C$	
Leaf trait	r	P	r	P
No. of connections per mesophyll plate	**0.9333**	0.0007	0.6980	0.0542
Width	−0.6144	0.1051	**−0.9317**	0.0008
Leaf length	−0.8000	0.0171	**−0.9293**	0.0008
Perimeter of cross section	−0.5419	0.1653	**−0.9123**	0.0016
Mesoporosity	**−0.8989**	0.0024	−0.8079	0.0153
Total cross-sectional area	−0.4628	0.2482	**−0.8884**	0.0032
Distance between mesophyll plates	−0.8678	0.0052	**−0.8829**	0.0037
Leaf mass per area	**0.8597**	0.0062	0.7714	0.0250
No. of mesophyll plates per mm	**0.8227**	0.0012	0.7944	0.0185
Stomatal pore index (SPI)	−0.2202	0.6003	**−0.4597**	0.2518
Guard cell length	−0.0928	0.8270	**−0.2430**	0.5620

distance between plates (Table 4, Fig. 4A). Parenchyma cells of the spongy mesophyll were plicate and connected at the plications in a way that left numerous airspaces between cells (Figs. 3C, 4B). Astrosclereids appeared frequently when leaves were examined in longitudinal section, especially in the upper crown. Arms of astrosclereids were flexible when sectioned green, bending when probed and then returning to their original shape, suggesting that they may be hygroscopic (Fig. 4C). The endodermis was typically thinner and not visibly suberized in the section closest to the xylem. In fresh leaves from tree 6, which had been collected during bud-swell, amyloplasts lined the periclinal cell walls (Fig. 4D). Guard cell length and stomatal pore index (SPI, guard cell length per leaf area) were unrelated to height or $\delta^{13}C$.

In a surprising contrast to our observations of *P. sitchensis* and *S. sempervirens* leaves, we observed abundant green-algal epiphylls in the genus *Protococcus* on *P. menziesii* at all heights, accumulating in the adaxial groove, stomatal beds, and furrows between epidermal cells (Figs. 3E, 4E: Bernstein and Carroll, 1977). These algae were present in our samples from both California and Washington, covering ~45% of the leaf surface on tree 6 (visually estimated % cover based on both surface imprints and transverse sections), totaling 2376 m^2 of algae on this tree alone. They were also equally abundant on *P. menziesii* leaves from an inland California forest that receives <43 cm of annual precipitation (A. Chin, personal observation). *Protococcus* is very sparse on *S. sempervirens* and *P. sitchensis* (A. Chin, personal observation), suggesting a high degree of host specificity as seen in other algae living on temperate conifer leaves (Lin et al., 2012). The unusual furrows between epidermal cells in *P. menziesii* appeared to facilitate algal colonization (Fig. 4E).

Relative plasticity

We found that *P. menziesii* leaves had the lowest within-crown phenotypic plasticity of the three tallest conifers, and overall weaker (or no) trait correlations with height and light availability (Fig. 5, Table 5). Its mean relative plasticity value (trees 1–5) was 0.32 compared to 0.55 for *S. sempervirens* and 0.54 for *P. sitchensis* across nine traits (Table 5). Leaf mass per projected area was the only leaf trait for which *P. menziesii* did not have the lowest relative plasticity among the three species (Table 5).

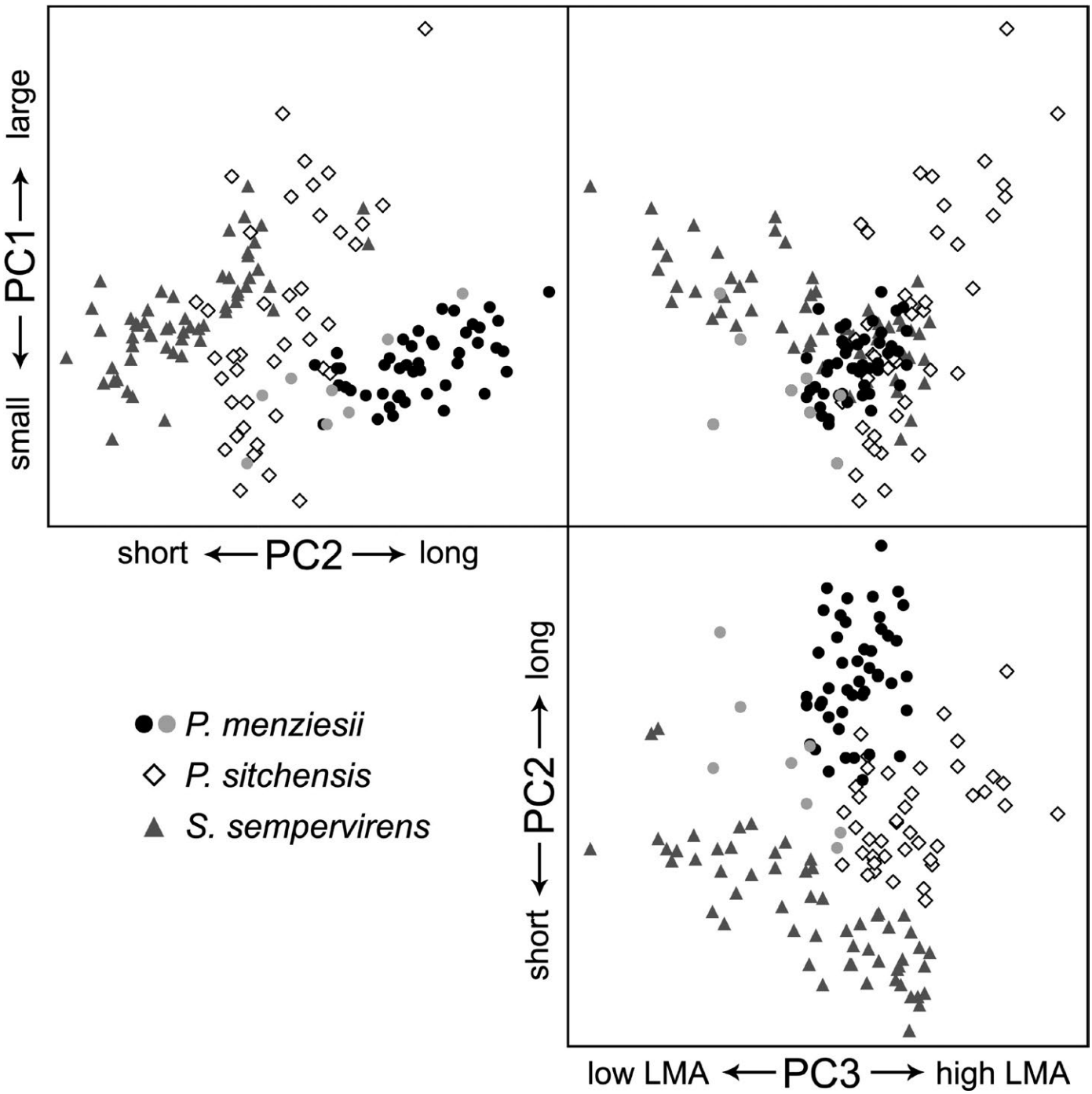

FIGURE 2. Plots of multi-species leaf PCA scores along the three significant axes, showing leaves from trees 1–5 as darker circles than those from tree 6, (*Picea sitchensis* data from Chin and Sillett, 2017; *Sequoia sempervirens* data from Oldham et al., 2010).

DISCUSSION

Leaves of *P. menziesii* vary anatomically and morphologically in response to the water-stress gradient induced by gravity, with little acclimation to light availability (Table 3). The best-explained leaf trait—LMA—is correlated with both height and $\delta^{13}C$; the next two best-explained traits—number of transfusion tracheids and cuticle thickness—are correlated only with height (Table 3). The conspicuous lack of variation in leaf width, which varies across the height gradient in other *P. menziesii* populations and in multiple other tall tree species (Fig. 2; Koch et al., 2004; Woodruff et al., 2008b; Chin and Sillett, 2017), is remarkable. Leaves of *P. menziesii* exhibit much less within-crown morphological and anatomical plasticity than the other two tallest conifers (Figs. 5, 6; Table 5).

Structural consistency of leaves may be supported by osmotic plasticity in response to the water-stress gradient or other ecological

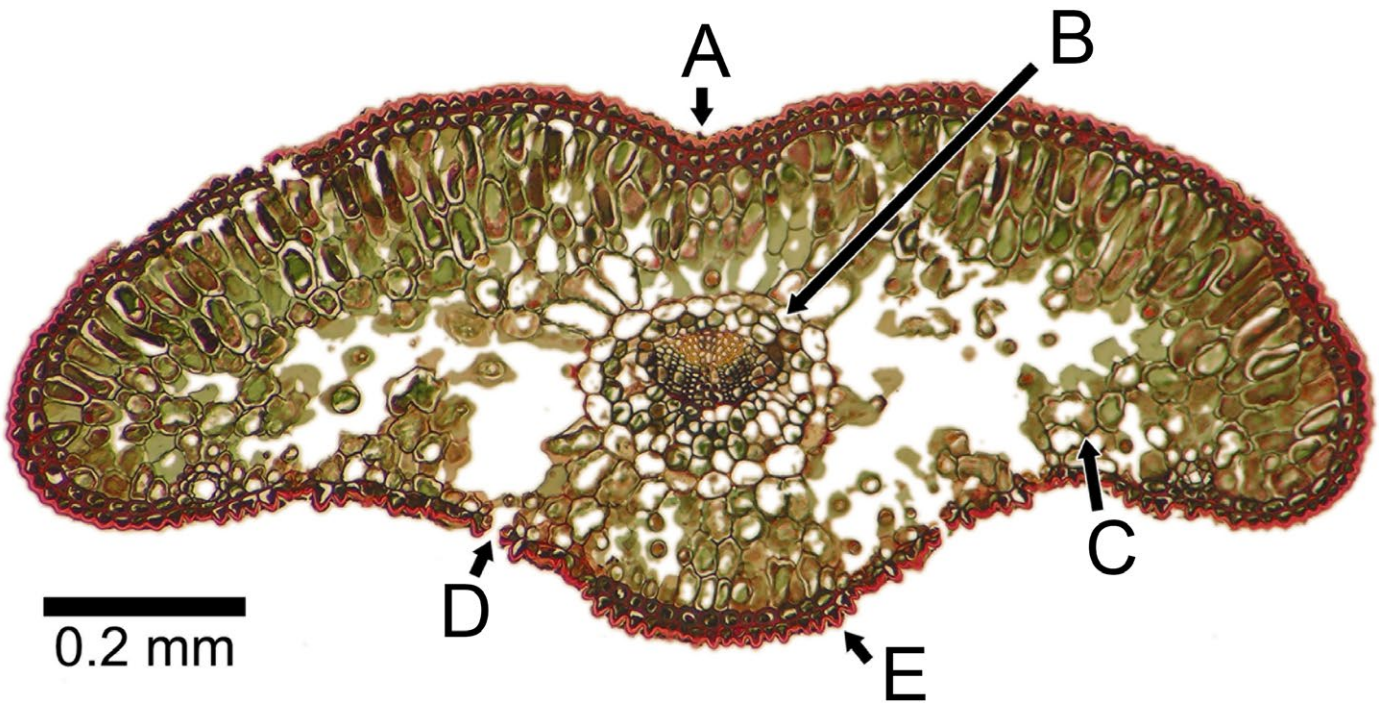

FIGURE 3. Stained transverse section of a *Pseudotsuga menziesii* leaf from mid-crown (70 m) showing (A) adaxial groove, (B) endodermis, (C) plicate mesophyll cell, (D) stoma, (E) strongly furrowed epidermis between stomatal beds. Within the boundaries of the endodermis, tracheids, in the transfusion tissue surrounding the vein, can be distinguished from parenchyma by empty lumens and orange-stained cell walls.

factors. Higher spring temperatures and solar angle, prevalence of coastal fog, or character displacement resulting from intense competition for light may induce more osmotic regulation of cell turgor during leaf elongation in *P. menziesii* of Prairie Creek Redwoods State Park than other forests. Differences in species composition and regional climate, particularly wind and storm intensity, may also be reflected in crown structure and leaf development. Tall individuals of *P. menziesii* in Washington, including tree 6, have denser crowns with many more leaves per unit crown volume than trees 1–5 of California, which are surrounded by taller and more shade-tolerant *S. sempervirens* (Sillett et al., 2018). Wind exposure enhancing water stress during leaf elongation in spring may also induce costs that

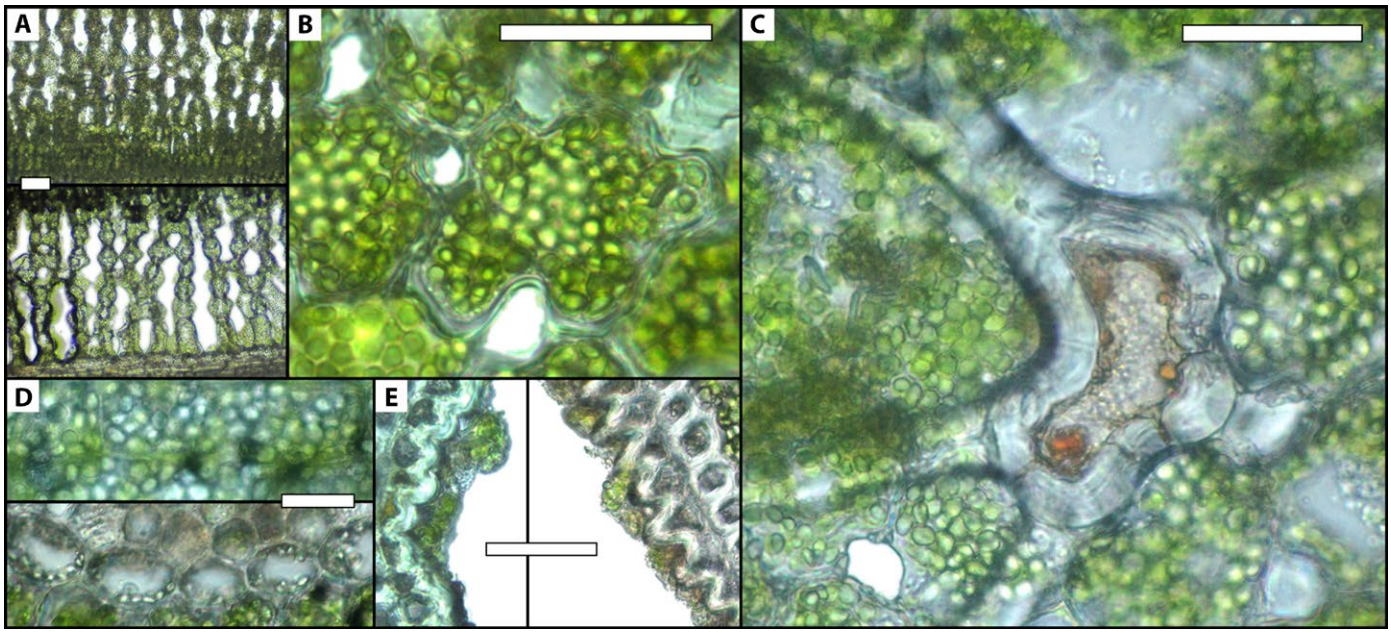

FIGURE 4. Fresh green sections of *Pseudotsuga menziesii* leaves showing (A) longitudinal sections through spongy mesophyll (90 m above, 20 m below), (B) mesophyll cells with airspaces between plications, (C) astrosclereid, (D) amyloplasts lining periclinal walls of endodermis (longitudinal section above, transverse section below), (E) epiphyllic algae (in adaxial groove on right, between stomatal beds on left). Scale bars = 30 µm.

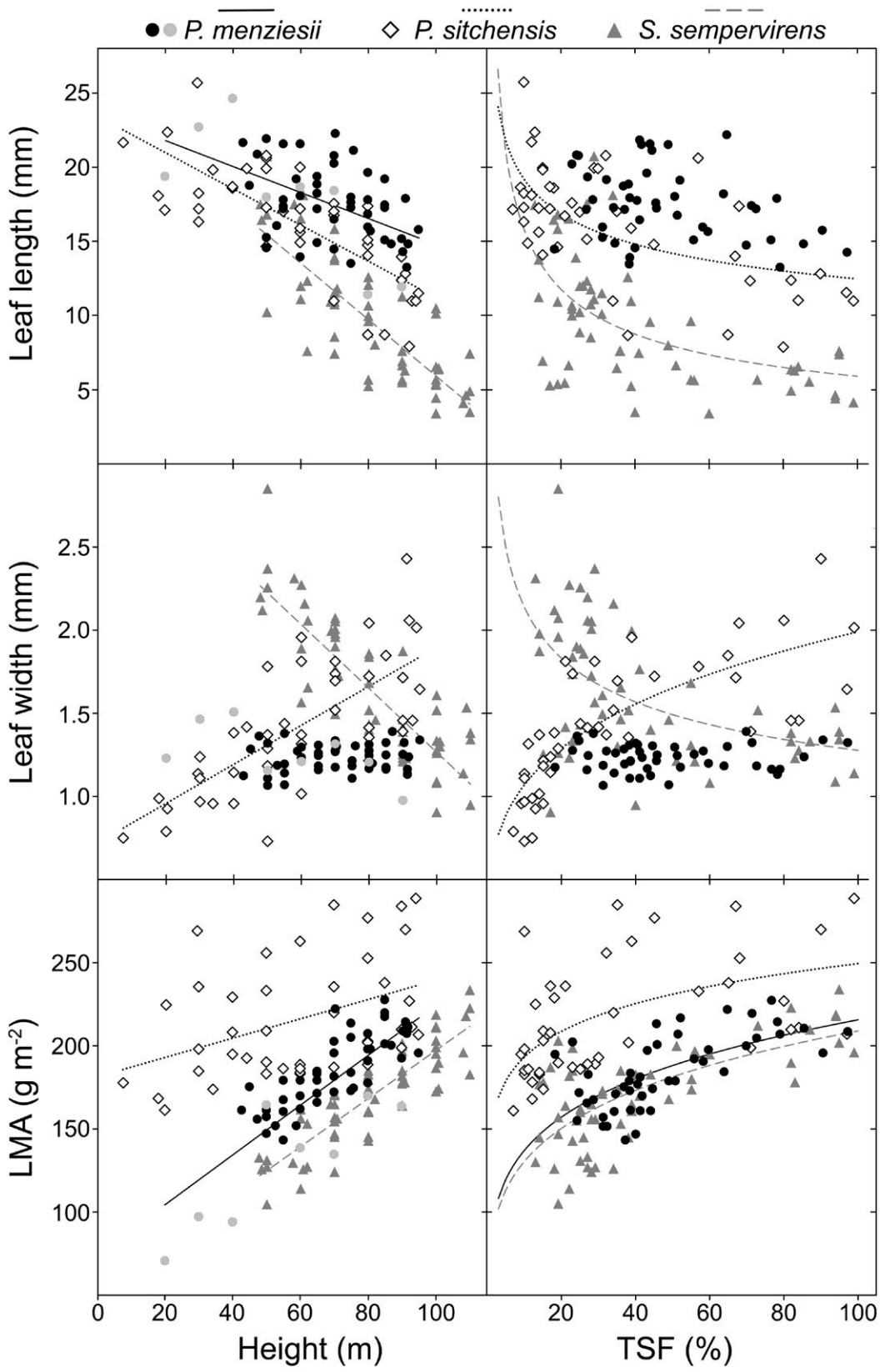

FIGURE 5. Scatterplots depicting how leaf structure of the three tallest conifers relates to height and light availability (TSF). Significant linear relationships to height and exponential relationships to light are shown (*Picea sitchensis* data from Chin and Sillett, 2017; *Sequoia sempervirens* data from Oldham et al., 2010).

TABLE 5. Relative plasticity values and correlations (*r*) with height for leaf traits of the three tallest conifer species. Data for *S. sempervirens* from Oldham et al. (2010) and *P. sitchensis* from Chin and Sillett (2017). All measurements, with the exception of leaf length and LMA, were made on transverse sections. *P. menziesii* = PSME (*N* = 46 leaves), *S. sempervirens* = SESE (*N* = 57 leaves), *P. sitchensis* = PISI (*N* = 42 leaves).

	Relative plasticity			Correlation with height		
Leaf trait	**PSME**	**PISI**	**SESE**	**PSME**	**PISI**	**SESE**
Area	0.31	0.64	0.36	0.33	0.66	−0.23
Perimeter	0.18	0.43	0.43	0.16	0.73	−0.83
Width	0.18	0.50	0.52	0.18	0.72	−0.80
Thickness	0.31	0.39	0.43	0.29	0.54	0.78
Xylem area	0.50	0.70	0.62	0.28	0.63	−0.66
Phloem area	0.53	0.70	0.72	0.31	0.61	−0.55
Transfusion tissue area	0.31	0.79	0.71	0.36	0.68	0.65
Leaf length	0.26	0.49	0.75	−0.40	−0.77	−0.81
Leaf mass per area	0.29	0.25	0.42	0.80	0.41	0.86

make maintaining long treetop leaves less feasible in Washington forests. In *P. menziesii*-dominated forests of Oregon, tall individuals of this species exhibit height-associated variation in leaf structure similar to what we observed in tree 6 (Woodruff et al., 2004, 2008a; Meinzer et al., 2008). Future work on leaf anatomy of *P. menziesii* would benefit from sampling more widely across its native geographic range, including *S. sempervirens*-dominated forests much farther south in California, where *P. menziesii* up to 90 m tall occur in mature, second-growth forests (Zane Moore, UC Davis, personal communication).

Hydraulic constraints on growth and acclimation to water stress

Gravity is inflexible in its impacts on Ψ, and while osmotic adjustments and foliar uptake of water may support both cell elongation and stomatal openness, reduced turgor with increasing height explains the consistent vertical gradient of increasing LMA within *P. menziesii* crowns (Fig. 5). The longest efficient length for *P. menziesii* leaves, before phloem would stagnate at the tip due to insufficient osmotic drive, is ~2.5 cm (based on mean phloem radius across trees 1–5, see Rademaker et al., 2017), which is similar to our observed maximum (2.2 cm) but considerably longer than our observed mean (1.8 cm) and minimum (1.3 cm) leaf lengths. In tree 6 from Washington, 86% of the variation in leaf length is explained by $\delta^{13}C$, a variable associated with the impacts of chronic water stress on stomatal and mesophyll CO_2 conductance (Table 4; Hultine and Marshall, 2000). Although the relationship between height and leaf length is weak in trees 1–5 ($R^2 = 0.16$), LMA of these trees is well explained by $\delta^{13}C$ ($R^2 = 0.69$, Table 3). The combination of increasing closeness and interconnectedness of mesophyll plates leads to lower mesoporosity in the upper crown and a strong negative correlation between mesoporosity and both height and $\delta^{13}C$ (Fig. 6, Table 4). Indeed, mesoporosity is the single best predictor of LMA in tree 6 ($R^2 = 0.90$). Among the three tallest conifers, LMA is the only one of nine leaf traits we considered for which *P. menziesii* does not have the lowest plasticity value or weakest correlation with height (Fig. 5, Table 5). Considering that phloem area is unrelated to height in any *P. menziesii* we examined, these patterns suggest that height-associated trends in LMA and leaf length are reflective of gravity's impacts on Ψ rather than acclimation to the light environment or limits set by decreasing phloem radii.

Our results highlight species-level differences in the degree to which gravity-induced water stress constrains leaf development. Height-related trends in leaf length observed in *P. menziesii* from California ($R^2 = 0.16$) are weaker than those in *S. sempervirens* ($R^2 = 0.65$) and *P. sitchensis* ($R^2 = 0.59$) from California (Fig. 5; Oldham et al., 2010; Chin and Sillett, 2017). Moreover, leaf length declines less steeply with height in *P. menziesii* from California (0.07 mm m^{-1}) than in *P. menziesii* from Washington (0.15 mm m^{-1}), *S. sempervirens* (0.19 mm m^{-1}), or *P. sitchensis* (0.12 mm m^{-1}). The hydraulically driven decrease in leaf length does not act on all cells equally, as stomatal guard cells become shorter with height in *S. sempervirens* ($R^2 = 0.61$) but not in *P. sitchensis* ($R^2 = 0.01$) or *P. menziesii* (data from tree 6, $R^2 = 0.01$, Chin and Sillett, 2017, and unpublished data, see Fig. 6). In both California and Washington, *P. menziesii* has the lowest LMA (as low as 163 g m^{-2} at 90 m), highest mesoporosity, longest leaves, and greatest mean phloem radius among the three tallest conifers (Oldham et al., 2010; Chin and Sillett, 2017). By some means not employed by the other species, *P. menziesii* decouples leaf elongation from the effects of gravity on Ψ, particularly in California where leaf length was weakly related to height.

In response to water stress, the number of tracheids in transfusion tissue of *P. menziesii* leaves increases with height, as does total vascular area and cuticle thickness (Table 3). While it is not surprising that the number of transfusion tracheids increases in *P. menziesii* by about 30% from the lower crown to the treetop, it is worth noting that total transfusion tissue area increases only slightly, suggesting that while cell numbers rise, area-based capacitance is unlikely to change in a physiologically meaningful way. The increase in tracheid numbers may indicate reduction in cell size, perhaps to prevent unrecoverable collapse in this flexible tissue, while the small increase in total area probably compensates for the additional cell wall fraction. Overall, *P. menziesii* has substantially less leaf-level phenotypic plasticity within its crowns than other conifers reaching heights >90 m with particularly low relative plasticity values and height correlations in traits associated with water-stress tolerance (Fig. 6, Table 5).

Strategic contrast within Pinaceae

Despite their familial relationship, endodermis, and plate-like mesophyll structure, leaf anatomical differences suggest that approaches to water transport outside the xylem diverged during evolution of *P. menziesii* and *P. sitchensis*. Transport of water through apoplastic pathways is enhanced by thick cell walls and a direct apoplastic route (Buckley et al., 2015), as seen in *P. sitchensis*, where the plicate cells of the mesophyll meet on the edges to form nearly straight radial paths from endodermis to ab- and adaxial stomata (Chin and Sillett, 2017). In contrast, mesophyll of *P. menziesii* appears to be better suited for vapor-phase water transport, as thin-walled mesophyll cells connect only on the crests of their plications, forming abundant airspaces at all heights and permitting airflow between plates but greatly adding to apoplastic tortuosity (Fig. 4B; Buckley et al., 2015). In addition to having a greater longitudinal mesoporosity, lower LMA, and more transfusion tissue than *P. sitchensis*, *P. menziesii* differs in having stomata only on the sheltered abaxial surface, which models suggest may promote water vapor diffusion down the leaf's internal temperature gradient (Fig. 3D; Rockwell et al., 2014; Buckley et al., 2015). Being hypostomatous is a trade-off

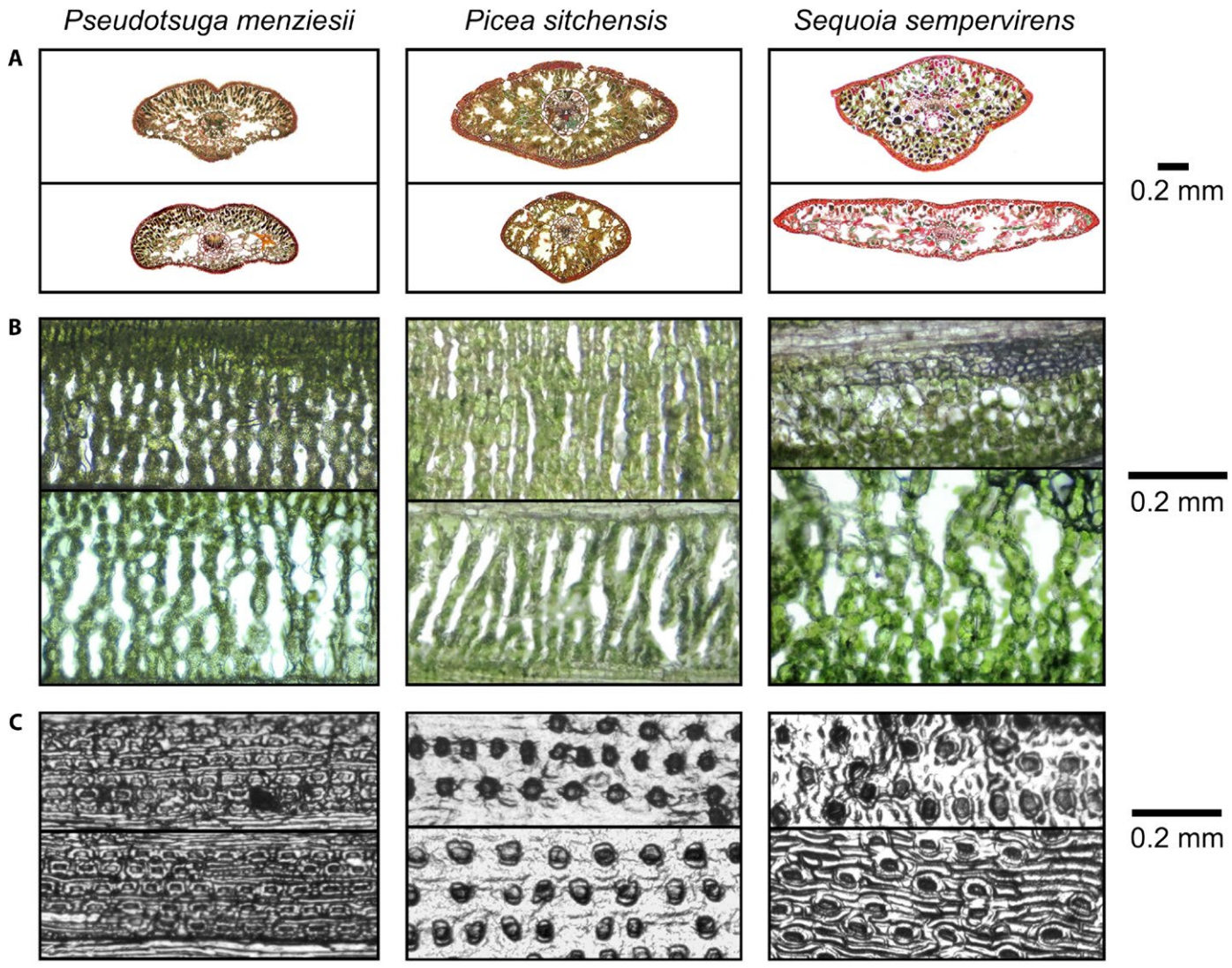

FIGURE 6. Anatomical responses to water stress and light availability gradients in the three tallest conifer species showing upper crown on top and lower crown on bottom of each row. (A) Stained leaf transverse sections: *Pseudotsuga menziesii*, 92 m and 45 m; *Picea sitchensis*, 95 m and 18 m; *Sequoia sempervirens*, 110 m and 48 m. (B) Fresh mesophyll longitudinal sections: *P. menziesii*, 90 m and 40 m; *P. sitchensis*, 92 m and 40 m; *S. sempervirens*, 110 m and 31 m. (C) Acrylic resin imprints of stomata: *P. menziesii*, 80 m and 40 m; *P. sitchensis*, 90 m and 34 m; *S. sempervirens*, 110 m and 31 m. All images within rows are at the same scale (bars on right).

for *P. menziesii*. Despite having less-dense mesophyll than *P. sitchensis*, *P. menziesii* leaves near the treetop have higher $\delta^{13}C$, indicating greater stomatal limitation of photosynthesis (Farquhar et al., 1989; Hultine and Marshall, 2000; Chin and Sillett, 2017). Nonetheless, vapor-phase transport is enhanced by solar radiation and can raise epidermal Ψ, perhaps making it a favorable strategy for a species whose geographic range extends into areas with abundant summer sun and high evaporative demand (Pieruschka et al., 2010; Peak and Mott, 2011; Rockwell et al., 2014; Buckley, 2015).

Astrosclereids, which are more frequent in leaves at the tops of tall trees than short ones, are a feature of *P. menziesii* absent from most other conifers, including *P. sitchensis* (Apple et al., 2002). Astrosclereids are flexible when fresh (but not when paraffin-embedded), concentrically lamellated, pored, and hollow with tannin inclusions (Fig. 4C). Visible lamellation and thickening of the S2 layer of the sclereid cell wall signifies the presence of cellulose and pectins, and thus water-holding capacity (Célino et al., 2013). These anatomical patterns suggest that astrosclereids could have an unrecognized hydraulic transport role as in fibers of *Gnetum gnemon* (Zwieniecki and Boyce, 2014) or enhance capacitance through increased apoplastic storage as in fibers of *S. giganteum*, both of which have structurally similar cell walls (Chin and Sillett, 2017; Williams et al., 2017). The means by which water is transported between vein and stomata determine most species-level variation in leaf hydraulic conductivity and, consequently, photosynthetic rate (Buckley, 2015; Scoffoni et al., 2016). Differences in traits related to variation in photosynthetic capacity under different environmental conditions are particularly relevant when considering that coast-restricted *P. sitchensis* is extraordinarily fast-growing in comparison to the longer-lived and wide-ranging *P. menziesii* (Kramer et al., 2018; Sillett et al., 2018). Substantial differences in leaf anatomy governing outside-xylem transport

separate *P. menziesii* from *P. sitchensis,* suggesting a mechanism by which leaf structure may influence species distribution and the composition of tall forests.

By investing in leaf length and mesoporosity, perhaps via increased production or use of osmoticum (Meinzer et al., 2008), tall *P. menziesii* trees pack high leaf area into upper crowns, which compensates for shade intolerance. Unlike neighbors, *P. menziesii* trees cannot maintain deep crowns in redwood rainforests unless standing near well-illuminated edges (Sillett et al., 2018), maybe because *P. menziesii* leaves acclimate less to environmental variation (Figs. 5, 6; Table 5). Even in tree 6 from Washington, where leaf structural variation was correlated with height, anatomical responses were of lesser magnitude than those in *P. sitchensis*, *S. sempervirens*, or *S. giganteum* (Oldham et al., 2010; Chin and Sillett, 2016, 2017). Although we can only speculate about their role, the potential contribution of the abundant epiphyllic algae to leaf water status and foliar uptake of water needs further study (Fig. 5E). Green algae do not require liquid water for rehydration, as they can access atmospheric moisture from as low as 68% relative humidity and maintain hydration via thick, mucilaginous cell walls (Tiffany, 1935; Mikhailyuk et al., 2003; Karsten et al., 2007). These algae also excrete extracellular polymeric substances that increase surface rugosity, decrease hydrophobicity, and increase water-binding capacity, causing surface moisture to stay elevated longer beneath algal films (Vázquez et al., 1998; Gaylarde and Morton, 1999; Karsten et al., 2007; Cutler et al., 2013). From a tree's perspective, having leaf surfaces that become moist without the presence of liquid water—and then stay moist for an extended period of time—could enhance water and nutrient trapping while promoting stomatal openness. Wet leaf surfaces lead to direct uptake of water and large increases in Ψ, with greater gains after an initial lag period, making prolonged wetness and rapid wettability physiologically valuable (Guzmán-Delgado et al., 2018). If nothing else, these algae contribute to forest primary productivity, capable of fixing >66 kg yr^{-1} of atmospheric C in tree 6 alone based on an annual C flux estimate of 28 g m^{-2} (Elbert et al., 2009).

CONCLUSIONS

Innate vertical gradients in crowns of tall conifers reveal several ways that leaves acclimate to environmental factors (Fig. 6). Gravity-induced water stress is consistently visible in leaves as low mesoporosity, high LMA, and elevated ^{13}C concentration near the tops of tall trees compared to lower in the crown. As in *S. sempervirens* but not *P. sitchensis*, leaf development in *P. menziesii* is more influenced by water stress than light availability, but its leaves exhibit less phenotypic plasticity in anatomical and morphological traits. Instead of physical variation, *P. menziesii* appears to have a third, alternative strategy where height-associated plasticity in osmotic adjustments (Meinzer et al., 2008) maintains sufficient turgor to produce relatively long leaves with high mesoporosity. Capacity to improve leaf water status in the face of low xylem Ψ may allow *P. menziesii* to minimize structural investments promoting either water-stress tolerance or acclimation to light availability. The restrained anatomical response to within-crown environmental gradients might maintain room in the design space of *P. menziesii* leaves, promoting greater climatic stress-tolerance, broader geographic range, and more diverse ecological associations. In nutrient-rich forests, light and treetop water are growth-limiting resources; thus, leaf-level traits involved in their acquisition and efficient use are points of divergence in the evolution of extraordinarily tall trees.

ACKNOWLEDGEMENTS

We thank R. Tate, S. McDonald, and S. Ruiz for assistance with sample preparation. We are grateful to A. Tomescu for advice and J. Freund for field assistance. We also thank editor C. Broderson and the anonymous reviewers for their helpful comments on the manuscript. Funding was generously provided by Kenneth L. Fisher, the National Science Foundation (IOB-0445277), and the Save the Redwoods League. We also thank the California Department of Parks and Recreation (Prairie Creek Redwoods State Park) and the National Park Service (Olympic National Park) for permission to conduct research in these reserves.

DATA ACCESSIBILITY

The three-species data set used to calculate phenotypic plasticity (Table 5) and in the PCA is publically available online at https://www.researchgate.net/publication/329254551_Vertical_gradients_in_leaf_anatomy_in_the_three_tallest_conifer_species?channel=doiandlinkId=5bff15e445851523d1531fe6andshowFulltext=true (https://doi.org/10.13140/RG.2.2.23654.88640). All other data are available from the authors upon request.

LITERATURE CITED

Ambrose, A. R., S. C. Sillett, and T. E. Dawson. 2009. Effects of tree height on branch hydraulics, leaf structure and gas exchange in California redwoods. *Plant, Cell and Environment* 32: 743–757.

Ambrose, A. R., W. L. Baxter, C. S. Wong, S. S. Burgess, C. B. Williams, R. R. Næsborg, G. W. Koch, and T. E. Dawson. 2016. Hydraulic constraints modify optimal photosynthetic profiles in giant sequoia trees. *Oecologia* 182: 713–730.

Apple, M., K. Tiekotter, M. Snow, J. Young, A. Soeldner, D. Phillips, D. Tingey, and B. J. Bond. 2002. Needle anatomy changes with increasing tree age in Douglas-fir. *Tree Physiology* 22: 129–136.

Azuma, W., H. R. Ishii, K. Kuroda, and K. Kuroda. 2015. Function and structure of leaves contributing to increasing water storage with height in the tallest *Cryptomeria japonica* trees of Japan. *Trees* 30: 1–12.

Bernstein, M. E., and G. C. Carroll. 1977. Microbial populations on Douglas fir needle surfaces. *Microbial Ecology* 4: 41–52.

Billow, C., P. Matson, and B. Yoder. 1994. Seasonal biochemical changes in coniferous forest canopies and their response to fertilization. *Tree Physiology* 14: 563–574.

Boyer, J. S. 1968. Relationship of water potential to growth of leaves. *Plant Physiology* 43: 1056–1062.

Boyer, J. S., and W. K. Silk. 2004. Hydraulics of plant growth. *Functional Plant Biology* 31: 761–773.

Brodribb, T. J., and N. M. Holbrook. 2005. Water stress deforms tracheids peripheral to the leaf vein of a tropical conifer. *Plant Physiology* 137: 1139–1146.

Buckley, T. N. 2015. The contributions of apoplastic, symplastic and gas phase pathways for water transport outside the bundle sheath in leaves. *Plant Cell and Environment* 38: 7–22.

Buckley, T. N., G. P. John, C. Scoffoni, and L. Sack. 2015. How does leaf anatomy influence water transport outside the xylem? *Plant Physiology* 168: 1616–1635.

Burgess, S. S. O., and T. E. Dawson. 2004. The contribution of fog to the water relations of *Sequoia sempervirens* (D. Don): foliar uptake and prevention of dehydration. *Plant, Cell and Environment* 27: 1023–1034.

Canny, M. J. 1993. Transfusion tissue of pine needles as a site of retrieval of solutes from the transpiration stream. *New Phytologist* 123: 227–232.

Carder, A. C. 1995. Forest giants of the world, past and present. Fitzhenry and Whiteside, Markham, Ontario, Canada.

Célino, A., S. Fréour, F. Jacquemin, and P. Casari. 2013. The hygroscopic behavior of plant fibers: a review. *Frontiers in Chemistry* 1: 43.

Cescatti, A., and R. Zorer. 2003. Structural acclimation and radiation regime of silver fir (*Abies alba* Mill.) shoots along a light gradient. *Plant Cell and Environment* 26: 429–442.

Chin, A. R. O., and S. C. Sillett. 2016. Phenotypic plasticity of leaves enhances water-stress tolerance and promotes hydraulic conductivity in a tall conifer. *American Journal of Botany* 103: 796–807.

Chin, A. R. O., and S. C. Sillett. 2017. Leaf acclimation to light availability supports rapid growth in tall *Picea sitchensis* trees. *Tree Physiology* 37: 1352–1366.

Chin, A. R. O., and S. C. Sillett. 2018. Vertical gradients in leaf anatomy in the three tallest conifer species. *A dataset*. https://doi.org/10.13140/RG.2.2.23654.88640

Cosgrove, D. J. 1993. How do plant cell walls extend? *Plant Physiology* 102: 1–6.

Cosgrove, D. J. 2000. Loosening of plant cell walls by expansins. *Nature* 407: 321–326.

Cutler, N. A., H. A. Viles, S. Ahmad, S. McCabe, and B. J. Smith. 2013. Algal 'greening' and the conservation of stone heritage structures. *Science of the Total Environment* 442: 152–164.

Elbert, W., B. Weber, B. Büdel, M. O. Andreae, and U. Pöschl. 2009. Microbiotic crusts on soil, rock and plants: neglected major players in the global cycles of carbon and nitrogen? *Biogeosciences Discussions* 6: 6983–7015.

Falster, D. S., and M. Westoby. 2003. Plant height and evolutionary games. *Trends in Ecology and Evolution* 18: 337–343.

Farquhar, G. D., J. R. Ehleringer, and K. T. Hubick. 1989. Carbon isotope discrimination and photosynthesis. *Annual Review of Plant Biology* 40: 503–537.

Gaylarde, C. C., and L. G. Morton. 1999. Deteriogenic biofilms on buildings and their control: a review. *Biofouling* 14: 59–74.

Gebauer, R. D., D. Volařik, J. Urban, I. Børja, N. E. Nagy, T. D. Eldhuset, and P. Krokene. 2011. Effect of thinning on anatomical adaptations of Norway spruce needles. *Tree Physiology* 31: 1103–1113.

Gebauer, R. D., D. Volařik, J. Urban, I. Børja, N. E. Nagy, T. D. Eldhuset, and P. Krokene. 2012. Effects of different light conditions on the xylem structure of Norway spruce needles. *Trees* 26: 1079–1089.

Gebauer, R. D., D. Volařik, J. Urban, I. Børja, N. E. Nagy, T. D. Eldhuset, and P. Krokene. 2015. Effects of prolonged drought on the anatomy of sun and shade needles in young Norway spruce trees. *Ecology and Evolution* 5: 4989–4998.

Guzmán-Delgado, P., J. M. Earles, and M. A. Zwieniecki. 2018. Insight into the physiological role of water absorption via the leaf surface from a rehydration kinetics perspective. *Plant, Cell and Environment* 41: 1886–1894.

Hardin, J., W. Leopold, and D. J. White. 2001. Harlow and Harrar's textbook of dendrology. 9th ed. University of Michigan, Ann Arbor, MI, USA.

Hu, Y. S., and B. J. Yao. 1981. Transfusion tissue in gymnosperm leaves. *Botanical Journal of the Linnean Society* 83: 263–272.

Hultine, K. R., and J. D. Marshall. 2000. Altitude trends in conifer leaf morphology and stable carbon isotope composition. *Oecologia* 123: 32–40.

Ishii, H. R., G. M. Jennings, S. C. Sillett, and G. W. Koch. 2008. Hydrostatic constraints on morphological exploitation of light in tall *Sequoia sempervirens*. *Oecologia* 156: 751–763.

Ishii, H. R., W. Azuma, K. Kuroda, and S. C. Sillett. 2014. Pushing the limits to tree height: Could foliar water storage compensate for hydraulic constraints in *Sequoia sempervirens*? *Functional Ecology* 28: 1087–1093.

Karsten, U., R. Schumann, and A. Mostaert. 2007. Aeroterrestrial algae growing on man-made surfaces. In J. Seckbach [ed.], Algae and cyanobacteria in extreme environments, 583–597. Springer, Berlin, Germany.

King, D. A. 1990. The adaptive significance of tree height. *American Naturalist* 17: 809–828.

Koch, G. W., S. C. Sillett, G. M. Jennings, and S. D. Davis. 2004. The limits to tree height. *Nature* 428: 851–854.

Kramer, R. D., S. C. Sillett, and R. Van Pelt. 2018. Quantifying aboveground components of *Picea sitchensis* for allometric comparisons among tall conifers in North American rainforests. *Forest Ecology and Management* 430: 59–77.

Liesche, J., H. J. Martens, and A. Schulz. 2011. Symplasmic transport and phloem loading in gymnosperm leaves. *Protoplasma* 248: 181–190.

Limm, E., K. Simonin, and T. Dawson. 2012. Foliar uptake of fog in the coast redwood ecosystem: a novel drought-alleviation strategy shared by most redwood forest plants. General Technical Report PSW-GTR-238: 263–271. Pacific Southwest Research Station, Forest Service, U.S. Department of Agriculture, Albany, CA, USA.

Lin, C.-S., Y.-H. Lin, and J-T. Wu. 2012. Biodiversity of the epiphyllous algae in a *Chamaecyparis* forest of northern Taiwan. *Botanical Studies* 53: 489–499.

Marshall, J. D., and R. A. Monserud. 2003. Foliage height influences specific leaf area of three conifer species. *Canadian Journal of Forest Research* 33: 164–170.

McCune, B., and M. J. Mefford. 2011. PC-ORD: Multivariate analysis of ecological data. MjM Software Design.

Meinzer, F. C., B. J. Bond, and J. A. Karanian. 2008. Biophysical constraints on leaf expansion in a tall conifer. *Tree Physiology* 28: 197–206.

Mikhailyuk, T. I., E. M. Demchenko, and S. Y. Kondratyuk. 2003. Algae of granite outcrops from the left bank of the river Pivdennyi Bug (Ukraine). *Biologia-Bratislava* 58: 589–602.

Niinemets, Ü. 2002. Stomatal conductance alone does not explain the decline in foliar photosynthetic rates with increasing tree age and size in *Picea abies* and *Pinus sylvestris*. *Tree Physiology* 22: 515–535.

Niinemets, Ü., and O. Kull. 1995a. Effects of light availability and tree size on the architecture of assimilative surface in the canopy of *Picea abies*: variation in needle morphology. *Tree Physiology* 15: 307–315.

Niinemets, Ü., and O. Kull. 1995b. Effects of light availability and tree size on the architecture of assimilative surface in the canopy of *Picea abies*: variation in shoot structure. *Tree Physiology* 15: 791–798.

Niklas, K. J. 1997. The evolutionary biology of plants. University of Chicago Press, Chicago, IL, USA.

Oldham, A. R., S. C. Sillett, A. M. Tomescu, and G. W. Koch. 2010. The hydrostatic gradient, not light availability, drives height-related variation in *Sequoia sempervirens* (Cupressaceae) leaf anatomy. *American Journal of Botany* 97: 1087–1097.

Peak, D., and K. A. Mott. 2011. A new, vapour-phase mechanism for stomatal responses to humidity and temperature. *Plant, Cell and Environment* 34: 162–178.

Peres-Neto, P. R., D. A. Jackson, and K. M. Somers. 2005. How many principal components? Stopping rules for determining the number of non-trivial axes revisited. *Computational Statistics & Data Analysis* 49: 974–997.

Pieruschka, R., G. Huber, and J. A. Berry. 2010. Control of transpiration by radiation. *Proceedings of the National Academy of Sciences, USA* 107: 13372–13377.

Rademaker, H., M. A. Zwieniecki, T. Bohr, and K. H. Jensen. 2017. Sugar export limits size of conifer needles. *Physical Review E* 95: 042402.1–8.

Rockwell, F. E., N. M. Holbrook, and A. D. Stroock. 2014. The competition between liquid and vapor transport in transpiring leaves. *Plant Physiology* 164: 1741–1758.

Sawyer, J. O., T. Keeler-Wolf, and J. Evens. 2009. Manual of California vegetation. California Native Plant Society Press, Sacramento, CA, USA.

Scoffoni, C., D. S. Chatelet, J. Pasquet-Kok, M. Rawls, M. J. Donoghue, E. J. Edwards, and L. Sack. 2016. Hydraulic basis for the evolution of photosynthetic productivity. *Nature Plants* 2: 16072.

Sillett, S. C., R. Van Pelt, R. D. Kramer, A. L. Carroll, and G. W. Koch. 2015. Biomass and growth potential of *Eucalyptus regnans* up to 100 m tall. *Forest Ecology and Management* 348: 78–91.

Sillett, S. C., R. Van Pelt, J. A. Freund, J. Campbell-Spickler, A. L. Carroll, and R. D. Kramer. 2018. Development and dominance of Douglas-fir in North American rainforests. *Forest Ecology and Management* 429: 93–114.

Tiffany, L. H. 1935. Algae of bizarre abodes. *Scientific Monthly* 40: 541–545.

Valladares, F., D. Sánchez-Gómez, and M. A. Zavala. 2006. Quantitative estimation of phenotypic plasticity: bridging the gap between the evolutionary concept and its ecological applications. *Journal of Ecology* 94: 1103–1116.

Van Pelt, R. 2001. Forest giants of the Pacific coast. Global Forest Society, Banff, AB, Canada.

Van Pelt, R., and S. C. Sillett. 2008. Crown development of coastal *Pseudotsuga menziesii*, including a conceptual model for tall conifers. *Ecological Monographs* 78: 283–311.

Van Pelt, R., S. C. Sillett, W. A. Kruse, J. A. Freund, and R. D. Kramer. 2016. Emergent crowns and light-use complementarity lead to global maximum biomass and leaf area in *Sequoia sempervirens* forests. *Forest Ecology and Management* 375: 279–308.

Van Volkenburgh, E., and J. S. Boyer. 1985. Inhibitory effects of water deficit on maize leaf elongation. *Plant Physiology* 77: 190–194.

Vázquez, G., P. Moreno-Casasola, and O. Barrera. 1998. Interaction between algae and seed germination in tropical dune slack species: a facilitation process. *Aquatic Botany* 60: 409–416.

Williams, C. B., R. Reese Næsborg, and T. E. Dawson. 2017. Coping with gravity: the foliar water relations of giant sequoia. *Tree Physiology* 37: 1312–1326.

Woodruff, D. R., and F. C. Meinzer. 2011. Water stress, shoot growth and storage of non-structural carbohydrates along a tree height gradient in a tall conifer. *Plant, Cell and Environment* 34: 1920–1930.

Woodruff, D. R., B. J. Bond, and F. C. Meinzer. 2004. Does turgor limit growth in tall trees? *Plant, Cell and Environment* 27: 229–236.

Woodruff, D. R., F. C. Meinzer, and B. Lachenbruch. 2008a. Height-related trends in leaf xylem anatomy and shoot hydraulic characteristics in a tall conifer: safety versus efficiency in water transport. *New Phytologist* 180: 90–99.

Woodruff, D. R., F. C. Meinzer, B. Lachenbruch, and D. M. Johnson. 2008b. Coordination of leaf structure and gas exchange along a height gradient in a tall conifer. *Tree Physiology* 29: 261–272.

Woodruff, D. R., F. C. Meinzer, and K. A. McCulloh. 2010. Height-related trends in stomatal sensitivity to leaf-to-air vapour pressure deficit in a tall conifer. *Journal of Experimental Botany* 61: 203–210.

Wu, Y., B. R. Jeong, S. C. Fry, and J. S. Boyer. 2005. Change in XET activities, cell wall extensibility and hypocotyl elongation of soybean seedlings at low water potential. *Planta* 220: 593–601.

Zhang, Y.-J., F. E. Rockwell, J. K. Wheeler, and N. M. Holbrook. 2014. Reversible deformation of transfusion tracheids in *Taxus baccata* is associated with a reversible decrease in leaf hydraulic conductance. *Plant Physiology* 165: 1557–1565.

Zimmermann, M. H. 1983. Xylem structure and the ascent of sap. Springer-Verlag, Berlin, Germany.

Zwieniecki, M. A., and C. K. Boyce. 2014. The role of cellulose fibers in *Gnetum gnemon* leaf hydraulics. *International Journal of Plant Sciences* 175: 1054–1061.